

Pulsed polarization spectroscopy with strong fields and an optically thick sample

Frank C. Spano

Department of Chemistry, Temple University, Philadelphia, Pennsylvania 19122

Kevin K. Lehmann

Department of Chemistry, Princeton University, Princeton, New Jersey 08544

(Received 7 October 1991)

The theory of pulsed polarization spectroscopy in the case of a saturating pump pulse and an optically thick sample is presented, both with and without inhomogeneous broadening. It is found that the molecular anisotropy produced by pumping an *R*- or *P*-branch transition is maximized by using a pulse whose flip angle is near 2π for the *M* component with the largest Rabi frequency. Calculations with no or extreme inhomogeneous broadening differ insignificantly. Such a pump pulse produces an anisotropy (and thus polarization rotation of the probe beam) of the opposite sign of that produced by weak-field excitation. Pulse-propagation calculations obtained by numerically solving the coupled Maxwell-Bloch equations demonstrate that there exist "stable-area" pulses, much like for a two-level system. The lowest such stable pulse produces a flip angle of 2.21π for the $M=0$ level and produces close to the maximum polarization anisotropy. This pulse still weakly excites the sample, and thus lengthens as it propagates to conserve area. The effective absorption coefficient, however, is much less than that for weak pulses. It is expected that such pulses should provide an order of magnitude or more sensitivity for polarization spectroscopy than that obtained with nonsaturating pulses.

PACS number(s): 33.10.Ev, 33.80.Be

I. INTRODUCTION

Double-resonance methods are among the most powerful techniques of molecular spectroscopy. The selectivity of double resonance allows complex and even unresolved spectra to be assigned. It also allows one to reach states inaccessible from thermally populated levels. While there are many methods for detecting double resonance, polarization spectroscopy (PS) is among the most sensitive [1–5]. In polarization spectroscopy, one creates a state-specific birefringence in a molecular sample, and then probes for transitions from the pumped molecules via polarization rotation of a probe beam. Like all double-resonance methods, it requires a near saturating pump power to perturb the sample measurably from equilibrium. But unlike a Lamb dip, one detects the signal through nearly crossed polarizers, and therefore the method is nearly background free. Thus PS can be much more sensitive than straight absorption when the probe-laser amplitude is limited by technical noise. This characteristic makes it particularly useful for experiments with pulsed lasers where there are large shot-to-shot instabilities [5]. One can expect a sensitivity increase on the order of the square root of the polarization extinction ratio.

The signal in PS comes from an anisotropic distribution of magnetic sublevels produced by a polarized pump laser. The theory for polarization spectroscopy presented up to now has considered the steady-state response of the molecular sample, as one has under cw excitation. This situation does not apply for most applications of polariza-

tion spectroscopy with pulsed lasers, where one usually works at pressures low enough to ensure that negligible relaxation occurs during a single pulse. For weakly saturating pulses, perturbation theory allows one to predict the size of the polarization signals, but such an analysis breaks down for strongly saturating fields that can be produced with pulsed lasers. It is the purpose of this paper to present an analysis for the polarization anisotropy produced by a Fourier-transform (FT) limited pump pulse in the limit of no relaxation, including pulse propagation effects in an optically thick sample. We present nonperturbative results that show large enhancements in the expected probe-field polarization rotation when strong pump pulses with flip angles on the order of 2π are used in an optically thick sample. This suggests that polarization spectroscopy with FT pulsed sources is potentially a more sensitive technique than has been previously recognized.

In Sec. II a brief description of the technique of polarization spectroscopy is given. In Sec. III the optical Bloch equations are presented in the limit of negligible relaxation. In Sec. IV the PS signal is calculated in both the optically thin and thick limits. A Maxwell equation is introduced to account for the nonlinear propagation of the strong pump pulse. Finally we summarize our findings in Sec. V.

II. BACKGROUND

Before embarking on the mathematical details let us consider the general experimental arrangement and

energy-level schemes in more detail. The goal of polarization spectroscopy is to obtain simplified, high-resolution spectra of the molecule under study. By simplified, we mean that (1) the pump pulse has selectively depleted a specific (J, K) ground-state rovibrational level and the probe pulse measures the P , Q , and R transitions from that level or (2) that an excited state has been selectively populated and the probe pulse measures the P , Q , and R transitions from that excited level. In the first scheme the pump and probe transitions share a common ground state while in the second scheme the excited state of the pump transition serves as the ground state for the probe transitions. We will be considered cases where the pump and probe share only one state in common, i.e., we are not pumping and probing on the same transition.

The experimental arrangement for polarization spectroscopy using linearly polarized light is briefly as follows. A strong, saturating, and linearly polarized (along the z axis) pump pulse enters the sample followed, at a short time delay later, by a weak (i.e., nonsaturating) probe pulse traveling in the same or the opposite direction and polarized at an angle of 45° relative to the pump. The transmitted probe light is then sent through a nearly crossed polarizer (aligned at 135°) and detected. Because the pump pulse induces a nonuniform M -dependent ground-state (and excited-state) population, the probe pulse undergoes unequal absorption in the x or z direction. This translates into a polarization rotation that is detected. The detected signal, in terms of the initial probe pulse intensity I_0 , the finite extinction ratio of the crossed polarizers ϵ , the sample thickness L , and the small angle at which the polarizers deviate from exact crossing θ_p , is given by [4]

$$I_s = I_0 \left\{ \epsilon + \theta_p^2 + \frac{1}{2} \theta_p (\alpha_z - \alpha_x) L + \frac{1}{4} [(\alpha_z - \alpha_x) L]^2 \right\}, \quad (2.1)$$

neglecting a small dispersive contribution that is proportional to the background birefringence of the sample windows. In practice, the windows are carefully squeezed to make this birefringence negligible. Its presence only affects the expected line shape, not the on-resonance signals we will be calculating below.

In what follows, we will be comparing and contrasting the optically thin and thick limits on the basis of the differential absorption of the x and z components of the probe electric field α_x and α_z , respectively. The signal scales as θ_p , while the background and thus technical noise scale as $\epsilon + \theta_p^2$. As a result, the signal to noise is optimized by choosing $\theta_p^2 = \epsilon$, i.e., uncrossing the polarizers until the background is just doubled.

III. OPTICAL BLOCH EQUATIONS

The optical Bloch equations, modified to account for the $2J+1$ degenerate rotational transitions in the rovibronic transition from a ground-state level J , describe how the pump and probe electromagnetic fields interact with an ensemble of rotating molecules. In what follows we assume a strong pump beam and a weak probe beam. For an optically thin sample the optical Bloch equations

suffice for the calculation of the polarization rotation; however, in an optically thick sample we need an additional (Maxwell) equation to describe the reradiation of the molecular polarization, which effects the propagation of the pump beam. This will be considered in Sec. IV. Let us first consider the interaction of the pump and probe beams with an optically thin sample.

A. Pump beam

We start by assuming the pump pulse (as well as the probe) has a temporal width much shorter than any dephasing or relaxation times of the molecular gas. We define the polarization axis of the pump beam to be the z axis and the wave vector to lie along the y axis. For a distribution of inhomogeneously broadened two-level absorbers, the interaction with an externally applied electromagnetic wave polarized in the z direction, $E(y, t) = \frac{1}{2} E_z(t) e^{i(ky - \omega t)} + \text{c.c.}$, is described by the optical Bloch equations. Within the rotating-wave approximation and neglecting relaxation they are

$$\begin{aligned} \frac{d}{dt} p_M^0(\Delta\omega, t) &= i\Delta\omega p_M^0(\Delta\omega, t) + i(\mu/\hbar) d(JKM, J_1KM) \\ &\quad \times E_z(t) w_M^0(\Delta\omega, t), \end{aligned} \quad (3.1a)$$

$$\begin{aligned} \frac{d}{dt} w_M^0(\Delta\omega, t) &= -(\mu/\hbar) d(JKM, J_1KM) \\ &\quad \times \text{Im}[E_z(t) p_M^0(\Delta\omega, t)]. \end{aligned} \quad (3.1b)$$

Here, μp_M^0 is the positive-frequency component of the slowly varying induced polarization of the $JKM \rightarrow J_1KM$ transition, where μ is the electronic-transition dipole moment between the ground state and the electronic excited state near resonance with the pump frequency and is assumed to lie along the principal molecular axis. The superscript "0" refers to the $\Delta M = 0$ selection rule. In the laboratory frame, the polarization density is equal to

$$\frac{1}{2(2J+1)} \sum_M \eta f_{JK} \mu p_M^0 e^{i(ky - \omega t)} + \text{c.c.},$$

where η is the density of absorbers and f_{JK} is the fraction of absorbers in the ground state JK at equilibrium. $\eta f_{JK} w_M^0 / (2J+1)$ is equal to the excited state ($J'KM$) population density minus the ground state (JKM) population density; w_M^0 ranges from -1 in the ground state to $+1$ in the excited state. The frequency detuning between an absorber with Doppler-shifted transition frequency ω_0 and the applied field frequency ω is given by $\Delta\omega = \omega_0 - \omega$, and we assume that the pump is tuned to the line center ω_0^c of the Gaussian inhomogeneous line shape of width σ , given by $g(\omega_0 - \omega_0^c) = g(0) \exp[-(\omega_0 - \omega_0^c)^2 / \sigma^2]$.

The direction-cosine matrix element $d(JKMJ', K'M')$ for a general $JKM \rightarrow J'K'M'$ transition is generally composed of several factors [6], i.e., $d(JKM, J'K'M') = \phi_{JJ'} \phi_{JKJ'} \phi_{JM'J'}$, which account for the orientation of μ with respect to the polarization vector of the external laser beam. A symmetric-top molecule with μ along the

TABLE I. The J , K , and M dependences of the various factors that comprise the transition dipole moment in a rotationally degenerate molecule.

	$J'=J-1$	$J'=J$	$J'=J+1$
$\phi_{JM' M}^z$	$2\sqrt{J^2-M^2}$	$2M$	$2\sqrt{(J+1)^2-M^2}$
$\phi_{JM' M\pm 1}^x$	$\pm\sqrt{(J\mp M)(J\mp M-1)}$	$\sqrt{(J\mp M)(J\pm M+1)}$	$\mp\sqrt{(J\pm M+1)(J\pm M+2)}$
$\phi_{JKJ'K}$	$2\sqrt{J^2-K^2}$	$2K$	$2\sqrt{(J+1)^2-K^2}$
$\phi_{JJ'}$	$(4J\sqrt{4J^2-1})^{-1}$	$[4J(J+1)]^{-1}$	$[4(J+1)\sqrt{(2J+1)(2J+3)}]^{-1}$

principal axis has the selection rules $\Delta K=0$, $\Delta J=0,\pm 1$, and $\Delta M=0,\pm 1$. Therefore, for a beam polarized along the z axis ($\Delta M=0$) the transition dipole moment for level M is $d(JKM, J'KM) = \mu\phi_{JJ'}\phi_{JKJ'K}\phi_{JM' M}^z$, while for an x polarized beam the dipole moment for the $M \rightarrow M+1$ transition is $d(JKM, J'KM+1) = \mu\phi_{JJ'}\phi_{JKJ'K}\phi_{JM' M+1}^x$. In both cases $J'=J, J\pm 1$. Table I contains all of the factors comprising $d(JKM, J'KM')$ for P , Q , and R transitions. We emphasize that the K dependence of the polarization signal appears only as a line strength scale factor, and the results which follow are independent of the direction of the transition moment in the molecular frame, or of whether the molecule is a symmetric or asymmetric top. Except for this overall line strength scaling, only the J values of the three levels are involved in double-resonance matter.

B. Probe beam

The weak probe pulse propagates along the y axis and is linearly polarized at 45° with respect to the pump pulse. Like the pump pulse, we assume that the probe pulse width is much shorter than any dephasing or damping time. If the pump beam is tuned to a $J \rightarrow J_1$ transition then the probe beam is tuned to a $J \rightarrow J_2$ transition ($J_2=J, J\pm 1$) in the common-ground-state level scheme, or to a $J_1 \rightarrow J_2$ transition ($J_2=J_1, J_1\pm 1$) in the excited-state absorption scheme. In both cases we have $J_1=J, J\pm 1$. A preferential absorption along the x or z axis results in an effective polarization rotation which is detected via transmission through a crossed polarizer aligned at 135° . The maximum signal is obtained when the probe pulse (like the pump pulse) is tuned to the inhomogeneous line center or to the molecules moving with zero velocity component along y . In the experiment, however, the probe beam is frequency scanned, and a line shape is recorded. Here, we calculate the peak of this line shape, and do not consider the more general case of arbitrary probe-beam detuning from line center.

Because the probe pulse is in the weak regime, we can neglect population transfer induced by the probe beam. This is justified when either the probe beam is much weaker than the pump or (the case of more experimental interest) the probe transition is much weaker than the pump transition, i.e., $\mu_p \ll \mu$, where μ_p is the probe transition dipole moment. Therefore a linearized version of Eq. (3.1) is used to calculate the probe absorption in each of the two polarization directions (x and z). Coherent interactions between the probe beam and the macroscopic polarization remaining in the wake of the pump pulse are unimportant if we assume that the probe-pump frequency

difference is much greater than the inhomogeneous transition linewidths.

IV. CALCULATION OF THE SIGNAL

We now proceed to calculate the polarization signal using the third term in Eq. (2.1) in the optically thin and thick limits.

A. Optically thin limit

Using Eqs. (3.1) to calculate the saturated population difference established by the pump pulse and the subsequent (weak) absorption of the two polarization components of the probe pulse, the differential absorption I_s for an optically thin sample of thickness L is calculated from Eq. (2.1) to be

$$I_s = -\frac{\kappa I_0}{J^2} \phi_{JKJ_2K}^2 \int_{-\infty}^{\infty} d\Delta\omega g(\Delta\omega) \mathcal{L}(\Delta\omega) \zeta_{JJ_1J_2}(\Delta\omega), \quad (4.1)$$

where I_0 is the input probe intensity integrated over time and $\kappa = \pi\eta f_{JK} \mu_p^2 \omega_0^2 L \theta_p / 2hc\epsilon_0$. $\mathcal{L}(\Delta\omega)$ is the normalized pulse excitation spectrum obeying $\int_{-\infty}^{\infty} d\Delta\omega \mathcal{L}(\Delta\omega) = 1$; in the case of Gaussian pump and probe pulses of full width (at $1/e$) $2t_p$, it is equal to

$$\mathcal{L}(\Delta\omega) = \frac{t_p}{\sqrt{2\pi}} e^{-(\Delta\omega t_p)^2/2}. \quad (4.2)$$

The anisotropy factor $\zeta_{JJ_1J_2}(\Delta\omega)$ in Eq. (4.1) is defined as

$$\zeta_{JJ_1J_2}(\Delta\omega) \equiv \frac{J^2 \phi_{JJ_2}^2}{2J+1} \sum_M [(\phi_{JM' J_2 M}^z)^2 - 2(\phi_{JM' J_2 M+1}^x)^2] \times N_{JJ_1 M}(\Delta\omega) \quad (4.3)$$

such that $\zeta_{JJ_1J_2}(\Delta\omega)$ converges for large J . $N_{JJ_1 M}(\Delta\omega)$ is the ground-state population prepared by the pump pulse, i.e., $N_{JJ_1 M} = \frac{1}{2}(1 - w_M^0)$. The anisotropy factor measures the effectiveness of the M -dependent ground- (or excited-) state population in rotating the probe-beam polarization. Generally, highly nonuniform distributions yield large anisotropy factors—a perfectly uniform ground-state population distribution gives $\zeta_{JJ_1J_2}(\Delta\omega) = 0$. Equations (4.1)–(4.3) apply to the common-ground-state arrangement. For the excited-state absorption scheme interchange J and J_1 and replace $N_{JJ_1 M}$ by the excited-state population $1 - N_{JJ_1 M}$, or just $-N_{JJ_1 M}$ since the summa-

tion of the constant 1 gives zero. Note that the sign of I_s reflects the sense of the probe-pulse polarization rotation.

Before continuing the analysis in the pulsed regime let us pause to consider the cw regime. The polarization signal for cw excitation can easily be calculated from the steady-state solutions of the Bloch equations (3.1) including relaxation terms [add the terms $-p_M^0(\Delta\omega, t)/T_2$ and $-(w_M^0(\Delta\omega, t)+1)/T_1$ to the right-hand side of Eqs. (3.1a) and (3.1b), respectively]. Using Eq. (2.1) the signal is found to have a form identical to Eq. (4.1) except that I_0 is replaced by the unintegrated probe intensity. In the steady-state limit the normalized pulse excitation function is given by

$$\mathcal{L}(\Delta\omega) = \frac{1}{\pi T_2} \frac{1}{\Delta\omega^2 + 1/T_2^2}, \quad (4.4)$$

where T_2 is the coherence relaxation time, which is assumed to be the same for both pump and probe transitions. The ground-state population prepared by the pump pulse in the cw case is equal to

$$N_{JJ_1M}(\Delta\omega) = \frac{1}{2} \left[1 + \frac{1}{1 + (\mu_M/\mu_{M_0})^2 (I/I_{\text{sat}}) (\pi/T_2) \mathcal{L}(\Delta\omega)} \right]. \quad (4.5)$$

Here we have $I/I_{\text{sat}} \equiv (\mu_{M_0} E_z / \hbar)^2 T_1 T_2$, where I is the intensity of the pump beam and I_{sat} is the saturation intensity for the transition with the maximum dipole moment $\mu_{M_0} = \mu d(JKM_0, J_1KM_0)$, i.e., $M_0 = 0$ for P and R transitions and $M_0 = J$ for Q transitions. In the cw limit the integration in Eq. (4.1) can be performed analytically, assuming that the inhomogeneous broadening is much greater than the homogeneous broadening ($\sigma \gg 1/T_2$), giving

$$I_s = -\kappa g(0) I_0 \frac{\phi_{JJ_2}^2 \phi_{JKJ_2K}^2}{2(2J+1)} \sum_M [(\phi_{JM_2M}^z)^2 - 2(\phi_{JM_2M+1}^x)^2] \times \frac{1}{\sqrt{1 + (\mu_M/\mu_{M_0}) I/I_{\text{sat}}}}. \quad (4.6)$$

In Fig. 1, we show the resonant anisotropy factor $\xi_{JJ_1J_2}(0)$ calculated by substituting Eqs. (4.4) and (4.5) into Eq. (4.3), as a function of I/I_{sat} for an R (50) pump transition ($J_1 = J + 1$) and a P (50) probe transition ($J_2 = J - 1$). The anisotropy is negative and has a maximum magnitude at $I/I_{\text{sat}} \approx 1$, after which it decreases to zero for large pump-beam intensities. This decrease is a result of strong saturation, where the ground-state population N_M approaches the value of $\frac{1}{2}$, independent of M ; a uniform distribution of ground- (or excited-) state population induces no polarization rotation in the probe beam. The negative sign of the anisotropy indicates that absorption is greater for the x component of polarization than for the z component. This is expected since the pump

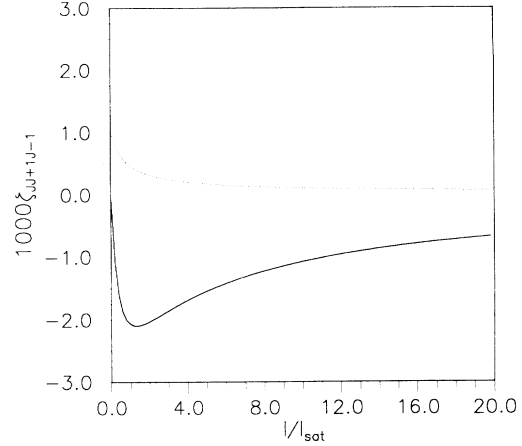


FIG. 1. $\xi_{JJ_1J_2}(0)$ as a function of I/I_{sat} for $J=50$ in the cw limit (solid curve). The dashed curve is the average population difference (over M). The anisotropy approaches zero as the population equalizes.

pulse at least partially saturates the transitions with low values of $|M|$, leading to reduced absorption of the z component of the probe beam.

Now let us return to the pulsed regime. For very short excitation pulses that satisfy $t_p \ll T^*$, where $T^* = 2/\sigma$ is the inhomogeneous dephasing time, the ground-state population established by the pump pulse becomes independent of $\Delta\omega$ and reduces to $N_M(\Delta\omega) = (1 + \cos\theta_M)/2$. The orientation-dependent pump-pulse area θ_M is defined as

$$\theta_M \equiv \frac{\mu}{\hbar} d(JKM, J_1KM) \int_{-\infty}^{\infty} E_z(t) dt. \quad (4.7)$$

The integral in Eq. (4.1) can now be easily evaluated. Using Eqs. (4.2), (4.3), and (4.7), the signal is calculated to be

$$I_s = -\frac{\kappa I_0 t_p}{J^2 \sqrt{2\pi}} \phi_{JKJ_2K}^2 \xi_{JJ_1J_2}(0), \quad \sigma t_p \ll 1 \quad (4.8)$$

with

$$\xi_{JJ_1J_2}(0) = \frac{J^2 \phi_{JJ_2}^2}{2(2J+1)} \sum_M [(\phi_{JM_2M}^z)^2 - 2(\phi_{JM_2M+1}^x)^2] \times (1 + \cos\theta_M). \quad (4.9)$$

Equations (4.8) and (4.9) also apply to the case of zero inhomogeneous broadening.

In the extreme-inhomogeneous-broadening limit there is also a simplification. Here $t_p \gg T^*$ so that $g(\Delta\omega)$ can be taken out of the integral in Eq. (4.1) as $g(0)$. The remaining integration in Eq. (4.1), however, must be performed numerically. In Fig. 2 we show $\xi_{JJ_1J_2}(0)$ from Eq. (4.9) as a function of the pulse area θ_0 for an R (50) pump transition ($J_1 = J + 1$) and a P (50) probe transition ($J_2 = J - 1$) in the short pulse limit (solid curve). Also shown is the average anisotropy in the extreme-inhomogeneous-broadening limit (dashed curve) given by $\int_{-\infty}^{\infty} d\Delta\omega \mathcal{L}(\Delta\omega) \xi_{JJ_1J_2}(\Delta\omega)$. As is evident, the two cases

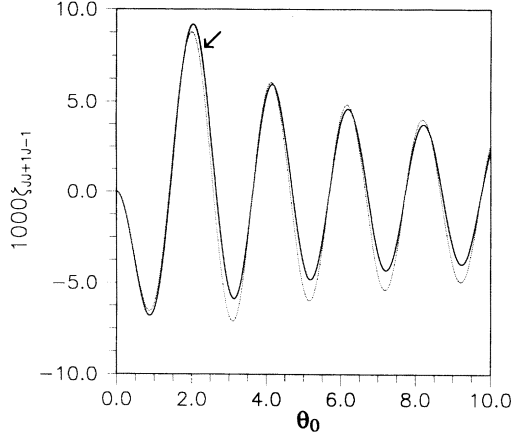


FIG. 2. $\zeta_{JJ_1J_2}(0)$ as a function of pulse area θ_0 and for $J=50$ with $J_1=J+1$ and $J_2=J-1$. The solid line corresponds to the short pulse limit [Eq. (4.9)] and the dashed line to the average anisotropy in the extreme inhomogeneous broadening limit (see text). Arrow indicates the first stable pump pulse area as calculated by setting the right-hand side of Eq. (4.12) to zero.

differ insignificantly; therefore in the extreme inhomogeneous broadening limit we have

$$I_s \approx -\frac{\kappa g(0)I_0}{J^2} \phi_{JKJ_2K}^2 \zeta_{JJ_1J_2}(0), \quad \sigma t_p \gg 1 \quad (4.10)$$

with the anisotropy factor of Eq. (4.9). $|\zeta_{JJ_1J_2}(0)|$ initially increases as θ_0^2 in the small-signal regime; as the saturation regime is approached $|\zeta_{JJ_1J_2}(0)|$ levels off (at $\theta_0 \approx \pi$) and then decreases to zero. Unlike the cw case, the anisotropy (and the signal) does not slowly approach zero as the pump intensity is increased; the behavior here is oscillatory with peak magnitudes at $\theta_0 \approx n\pi$ ($n=1, 2, \dots$) and zeros placed in between. Note that the magnitude of the anisotropy factor $\zeta_{JJ_1J_2}(0)$ in the pulsed regime is approximately three times larger than the cw value at the first minimum ($\theta_0 \approx \pi$) and approximately five times larger at the first maximum ($\theta_0 \approx 2\pi$). Similar oscillatory behavior exists when the pump beam is tuned to a P or Q transition. The reason for additional peaks for $n > 1$ can be seen in Fig. 3, which shows the ground-state population as a function of M in the unsaturated regime at $\theta_0 = \pi/4$, near the first minimum at $\theta_0 = \pi$ and near the first maximum at $\theta_0 = 2\pi$. As is evident, the ground-state population in the last case is the least uniform, resulting in the largest value for $\zeta_{JJ_1J_2}$. The sign change in $\zeta_{JJ_1J_2}(0)$ between the $\theta_0 = \pi$ and 2π cases is associated with the shift in the peak excited-state population from low $|M|$ values ($\theta_0 < 3\pi/2$) to high $|M|$ values ($3\pi/2 < \theta_0 < 5\pi/2$). The sign of the polarization rotation is therefore expected to change as one increases the pump pulse area in this regime.

We can directly compare the pulsed regime where $t_p \gg T^*$ with the cw regime. Using Eqs. (4.10) and (4.9) the maximum signal in the pulsed regime is approximately

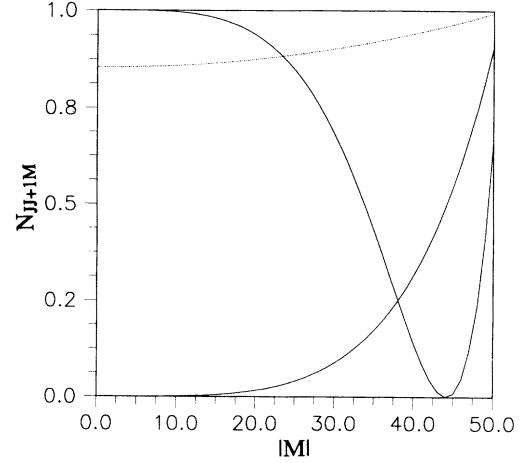


FIG. 3. Ground-state population at $\Delta\omega=0$ as a function of $|M|$ for a $R(50)$ transition for three values of the pump pulse area: $\theta_0 = \pi/4$ (dashed curve), $\theta = \pi$ (solid curve rising to the right), and $\theta = 2\pi$ (solid curve with a dip near $M = 45$).

$$I_s^{\max} \approx -9 \frac{\kappa g(0)I_0}{J^2} \phi_{JKJ_2K}^2$$

obtained when $\theta_0 = 2\pi$. In the cw limit the maximum signal is

$$I_s^{\max} \approx 2 \frac{\kappa g(0)I_0}{J^2} \phi_{JKJ_2K}^2,$$

obtained using Eq. (4.6) when $I/I_{\text{sat}} \sim 5$. The difference is due to the more anisotropic M -dependent population (ground or excited) induced in the pulsed regime (see Fig. 3). In the short (pump and probe) pulse regime ($t_p \ll T^*$) the maximum signal is reduced from the extreme inhomogeneous case by a factor of about t_p/T^* . This reduction is due to the fact that, in this limit, most of the probe photons are outside the absorption bandwidth and hence do not contribute to the signal.

B. Optically thick limit

In the optically thick limit pulse propagation effects become very important. For a nondegenerate two-level absorber, such as an atomic gas, there exist a wide variety of highly nonlinear propagation effects such as pulse splitting and steepening and self-induced transparency (SIT) [7]. The latter phenomenon is characterized by a stable hyperbolic-secant pulse shape of area $\theta = 2\pi$ which travels without absorption or reshaping, but with reduced velocity, through an optically thick sample. The pulse is one solution to the coupled Maxwell-Bloch equations which admits stable solutions for pulse areas of $2n\pi$ ($n=0, 1, 2, \dots$) and unstable solutions for $\theta = (2n+1)\pi$. The instability manifests itself in the high sensitivity of the pulse evolution to input areas near $\theta = (2n+1)\pi$; a pulse with an input area slightly smaller than π , for example, will undergo attenuation to a zero area, while a pulse with an input area slightly greater than π will evolve into the stable hyperbolic-secant solution with

area 2π . This behavior was first discovered by McCall and Hahn [7] and is formulated mathematically in what is commonly referred to as the area theorem. The effects of rotational degeneracy on pulse propagation and SIT has been studied extensively in the late 1960s to the mid 1970s by several groups both theoretically and experimentally using SF_6 [8,9]. Gibbs, McCall, and Salamo [9] showed that the propagation of a linearly polarized laser pulse behaves in many ways like nondegenerate SIT when tuned to a P or R transition but not to a Q transition. Hopf, Rhodes, and Szoke [10] studied the propagation of pulses tuned to a Q transition.

For spectroscopic purposes, SIT in nondegenerate two-level systems (TLS) is not very useful since no light is absorbed; this is not the case for $\theta_{M_0}=2\pi$ pulses in rotationally degenerate TLS, where absorption (or stimulated emission) occurs for the $\Delta M=0$ transitions when $M \neq M_0$. The propagation of the pump pulse through a medium of rotationally degenerate two-level systems is governed by the Maxwell equations; in the plane-wave limit and for a field on resonance, they reduce to a single equation [8–10]:

$$\frac{\partial}{\partial \xi} E_z(\xi, t) = \frac{\hbar}{2\pi g(0)\mu\sigma_{JKJ,K}} \times \sum_M d(JKM, J_1KM) \times \int_{-\infty}^{\infty} g(\Delta\omega) \text{Im}[p_M^0(\Delta\omega, t)] d\Delta\omega \quad (4.11)$$

for a plane polarized pulse in the z direction with y being the propagation direction. Here

$$\sigma_{JKJ,K} \equiv \sum_M d(JKM, J'KM)^2$$

and $\xi = \alpha y$, where α is the Beer's law absorption length for the medium. Equation (4.11) leads directly to an area theorem, generalized to include the rotationally degenerate $\Delta M=0$ transitions [8–10]:

$$\frac{\partial}{\partial \xi} \theta(\xi) = - \frac{\mu_{M_0}}{2\mu\sigma_{JKJ,K}} \sum_M d(JKM, J_1KM) \sin\theta_M(\xi), \quad (4.12)$$

where the maximum transition dipole is $\mu_{M_0} = \mu d(JK0, J_1K0)$ and $\mu d(JKJ, J_1KJ)$ for a P (or R) branch and Q branch transition respectively, and where $\theta \equiv \theta_{M_0}$. For a nondegenerate transition Eq. (4.12) reduces to the standard area theorem originally derived by McCall and Hahn [7]. In this case area and pulse-shape conserving solutions exist for $\theta = 2n\pi$ ($n=1, 2, \dots$). Unstable solutions exist at $\theta = (2n+1)\pi$. For rotationally degenerate two-level systems, the stable (and unstable) area conserving solutions exist at the zeros of the right-hand side of Eq. (4.12). One can demonstrate numerically that the stable solutions are shifted from $2n\pi$ and the unstable solutions are shifted from $(2n+1)\pi$. In the large- J limit, the first unstable

solution of Eq. (4.12) is $\theta = 1.15\pi$ for a P (or R) transition and $\theta = 1.43\pi$ for a Q transition. The first stable solutions are at $\theta = 2.21\pi$ for P or R transitions and at $\theta = 2.46\pi$ for the Q transition [8,9]. Thus for a high- J , P transition, the area of a pulse which is initially slightly less than 1.15π will tend to zero at large propagation distances. If the input area is slightly greater than 1.15π , the pulse area will evolve to a constant value of 2.21π . Because of the distribution in transition moments, there is absorption and pulse reshaping even though the area is conserved by Eq. (4.12). The polarization from some M components ($\pi < \theta_M < 2\pi$) tends to increase the pulse area, while the others tend to decrease it, leading to a net cancellation at the stable area. We have confirmed this behavior numerically by integrating the Maxwell-Bloch equations over space and time using standard numerical algorithms [11]. Figure 4(a) shows the pulse area θ as a function of ξ for a laser pulse tuned to a $P(9)$ transition (solid curves) and a $Q(9)$ transition (dashed curves) for several values of the initial pulse area. The input envelope is taken to be Gaussian, $E_z(t) = E_0 \exp[-(t/t_p)^2]$. When the initial area is above the first unstable solution but below the first stable solution, the area evolves toward the stable value, which is 2.22π and 2.32π for the $P(9)$ and $Q(9)$ transitions, respectively. [The $R(9)$ solution is practically indistinguishable from the $P(9)$ solution.] These values are already close to the high- J values. Note that for small input areas, the area decays exponentially to zero like $\exp[-\alpha y/2]$, which is the linear Beer's law result. Consideration of the normalized pulse energies (integrated over time) shown in Fig. 4(b) reveals that a much smaller fraction of the pulse energy is absorbed per unit length for the initial pulse areas near the stable solution. This is due to the restricted range of M values that are strongly pumped by this pulse. By referring to Fig. 2, however, we also find that these stable pulse areas yield high values for $\zeta_{JJ+1J-1}$ and hence nearly maximize the signal in polarization spectroscopy. The increase in signal can be substantially greater than in the unsaturated regime because molecules over many Beer's lengths can interact with the probe pulse.

In Table II, we collect our findings for the two energy-level schemes. The convergent value of $\zeta_{JJ_1J_2}$ for large J values is tabulated for all of the nine possible transitions in the common-ground-state scheme. $\zeta_{JJ_1J_2}$ is evaluated at the first stable pulse area ($P, R: 2.21\pi; Q: 2.46\pi$) for the pump pulse using Eq. (4.10). To obtain the excited-state absorption results, relabel the rows as $J_2 = J_1 - 1, J_1$

TABLE II. Calculated values of $10^3 \zeta_{JJ_1J_2}(0)$ from Eq. (4.9) in the large- J limit ($J=1000$) and for the common-ground-state configuration. In the excited-state absorption configuration simply change the sign.

	$J_1 = J - 1$	$J_1 = J$	$J_1 = J + 1$
$J_2 = J - 1$	7.6	-4.0	7.6
$J_2 = J$	-31	16	-31
$J_2 = J + 1$	7.6	-4.0	7.6

and $J_1 + 1$ and change the sign of $\zeta_{JJ_1J_2}$. Substitution of these values into Eq. (4.1) gives the polarization signal in the high optical density limit with strong laser pulses. Tables similar to Table II can be constructed for the higher stable solutions, but consideration of Fig. 2 shows the first stable solution to give the maximum signal.

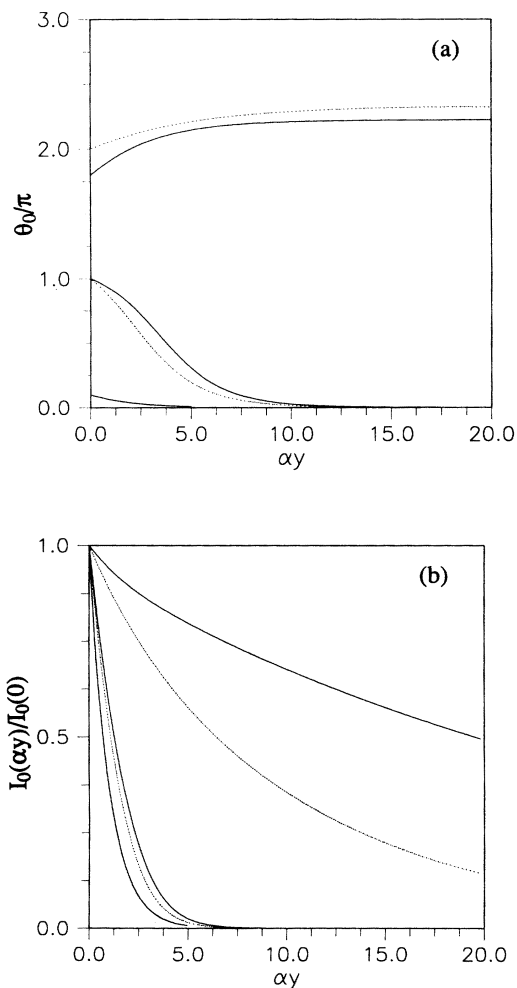


FIG. 4. (a) Pulse-pulse area as a function of αy . The pump is tuned to a $R(9)$ (solid curve) and $Q(9)$ (dashed curve) transition in the extreme inhomogeneous broadening limit. The curves were obtained by numerically integrating the coupled Maxwell-Bloch equations [Eqs. (3.1) and (4.11)]. Three input areas are shown: the top curves correspond to $\theta_0 = 2\pi$ and 1.8π for the R and Q cases, respectively. Note the increase in pulse area to the stable propagation values predicted by the area theorem. The middle curves have $\theta_0 = \pi$ and the lower curves have $\theta_0 = 0.1\pi$. In these cases the initial pulse area is below the first unstable value so the area decays to zero. In (b) the normalized pulse intensities (integrated over time) are shown for all three cases. The propagation depths of the higher area pulses are much greater allowing more absorbers to contribute to the signal. Note that the case with $\theta_0 = 0.1\pi$ obeys Beer's law (the Q and R cases completely overlap and cannot be distinguished in the figure).

V. CONCLUSION

We have presented a nonperturbative approach to calculating the probe-pulse polarization rotation in polarization spectroscopy for an arbitrarily optically thick medium. The generality of the approach leads to several interesting phenomena.

(1) In the optically thin limit, a pump pulse, which is shorter than any system relaxation time, induces a sample birefringence that is several times greater than that established using cw beams. The birefringence is an oscillatory function of the pump pulse area (calculated with respect to the M_0 transition, where $M_0 = 0$ for P or R transitions, and $M_0 = J$ for Q transitions), with maxima occurring at integral multiples of π . At odd multiples the polarization rotation is positive while at even multiples it is negative.

(2) In optically thick samples, where the reradiated field of the medium is no longer negligible compared to the pulse field, Maxwell's equation is needed to describe the pump-pulse propagation. In a rotationally degenerate medium the propagation obeys a generalized area theorem, which predicts that the pump pulse area converges to a stable value as it propagates. Surprisingly this value is very close to 2π , the value which maximizes birefringence in the optically thin limit. The solitonlike pump pulse is thus capable of inducing the same near-optimal anisotropy to all resonance absorbers at depths much greater than the Beer's length. In this way many more absorbers can contribute in an optimal way to the signal. This holds great promise for observing weak probe transitions since the signal may then be increased by orders of magnitude.

Although the pulse area converges to a stable value, the pulse shape is not preserved, as in nondegenerate self-induced transparency. In order to establish the nonuniform M -dependent ground- and excited-state populations the pulse must be absorbed to some extent. Figure 5 shows the pulse shape for a $R(9)$ pump pulse at three distances into the absorber in the extreme inhomogeneous broadening limit. To maintain constant area while losing energy due to absorption, the pulse width increases with propagation distance, and the ground state hole in the broad inhomogeneous band therefore narrows with propagation distance. Thus the M -dependent excited-state population, which leads to the near-optimal birefringence, is maintained for a decreasing number of adsorbers as the pulse travels further into the medium. As the pulsewidth approaches the excited and ground state population and coherence relaxation lifetimes, Equations (3.1) are no longer valid and the additional relaxation terms must be included. For pulse widths approaching the relaxation lifetimes the area theorem breaks down; if the distance at which this happens is defined as L_c , then when $y > L_c$ the near-optimal birefringence will no longer be maintained. However, by choosing a sufficiently short pump pulse, most of the pulse energy is absorbed before the pulse reaches L_c and L_c may be several orders of magnitude greater than the Beer's absorption length (see Fig. 4).

As a potential application of these ideas, consider the

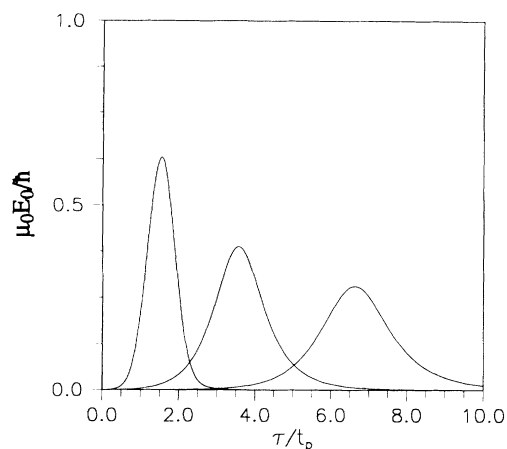


FIG. 5. Electric-field envelope at three distances into the absorber: $\alpha y = 0.2, 10,$ and 20 for an initial Gaussian pulse of $(1/e)$ full width $2t_p$, calculated by numerically integrating the Maxwell-Bloch equations [Eqs. (3.1) and (4.10)] in the extreme inhomogeneous broadening limit. Pulse frequency is tuned to a $R(9)$ transition frequency. Pulses further to the right correspond to the higher propagation depths. Note the temporal broadening with propagation. Also note that the pulse travels slower than the speed of light in the material $v = c/n$, where n is the index of refraction and c is the speed of light in vacuum.

spectrum of methane. The overtone bands in the near infrared and visible are quite complex, and could not be assigned by traditional spectroscopic techniques. Recently, DeMartino and co-workers [12,13] have been able to assign the principal bands with two and three quanta of CH stretch by double resonance, using a pump-probe tech-

nique. Polarization spectroscopy would be expected to increase the sensitivity of these experiments by several orders of magnitude, allowing the higher bands (which are of importance in planetary astronomy) to be studied. With a FT-limited pump pulse, one can achieve a 10-nsec " 2π " pulse on the ν_3 fundamental near $3.3 \mu\text{m}$ with a fluence of on the order of $100 \mu\text{J}/\text{cm}^2$. The strong lines in the ν_3 fundamental have peak absorption strengths on the order of $0.1\text{--}0.5 \text{ cm}^{-1} \text{ Torr}^{-1}$ and thus with a pressure on the order of 1 Torr (which will still have a relaxation rate slow compared with the pulse width) we will absorb a weak pulse in a few centimeters of pathlength. With such a small effective pathlength, sensitivity would be severely limited. However, by using a 2π pulse, we can use a factor of 10 or more longer pathlengths. Combined with the increased anisotropy of the sample, a large increase in sensitivity should result. An added benefit results from the decreasing spectral width of pumped molecules as the beam propagates through the sample. Without pulse reshaping, the spectral resolution of the probe transition is limited to the FT width of pump laser times the ratio of frequencies, due to the Doppler broadening. But as the 2π pulse propagates in the optically dense sample, it will lengthen in time and pump an even narrower distribution in velocity, leading to enhanced resolution on the pump transition.

ACKNOWLEDGMENTS

We would like to thank Joseph Eberly and Warren Warren for helpful discussions on this topic. Financial support was provided by Temple University and the National Science Foundation.

-
- [1] C. Weiman and T. Hansch, *Phys. Rev. Lett.* **36**, 1170 (1976).
 - [2] M. E. Kaminsky, R. T. Hawkins, F. V. Kowalski, and A. L. Schawlow, *Phys. Rev. Lett.* **36**, 671 (1976).
 - [3] R. Teets, R. Feinberg, T. W. Hansch, and A. L. Schawlow, *Phys. Rev. Lett.* **37**, 683 (1976).
 - [4] R. E. Teets, F. V. Kowalski, W. T. Hill, N. Carlson, and T. W. Hansch, *SPIE Laser Spectrosc.* **113**, 80 (1977).
 - [5] D. Frye, H. T. Liou, and H. L. Dai, *Chem. Phys. Lett.* **133**, 249 (1987).
 - [6] C. H. Townes and A. L. Schawlow, *Microwave Spectroscopy* (Dover, New York, 1975).
 - [7] S. L. McCall and E. L. Hahn, *Phys. Rev.* **183**, 457 (1969).
 - [8] C. K. Rhodes and A. Szoke, *Phys. Rev.* **184**, 25 (1969); P. K. Cheo and C. H. Wang, *Phys. Rev. A* **1**, 225 (1970); A. Zembrod and Th. Gruhl, *Phys. Rev. Lett.* **27**, 287 (1971).
 - [9] H. M. Gibbs, S. L. McCall, and G. J. Salamo, *Phys. Rev. A* **12**, 1032 (1975).
 - [10] F. A. Hopf, C. K. Rhodes, and A. Szoke, *Phys. Rev. B* **1**, 2833 (1970).
 - [11] A. Iosevigi and W. E. Lamb, Jr., *Phys. Rev.* **185**, 517 (1969).
 - [12] A. DeMartino, R. Frey, and F. Pradere, *Chem. Phys. Lett.* **95**, 200 (1983).
 - [13] M. Chevalier and A. DeMartino, *Chem. Phys. Lett.* **135**, 446 (1987).